Static Properties of Laser Welded Ultra-High-Strength Stainless Steel Tube

Mikko Hietala
Kerttu Saalasti Institute
University of Oulu
Nivala, Finland
mikko.hietala@oulu.fi

Markku Keskitalo
Kerttu Saalasti Institute
University of Oulu
Nivala, Finland
markku.keskitalo@oulu.fi

Antti Järvenpää
Kerttu Saalasti Institute
University of Oulu
Nivala, Finland
antti.jarvenpaa@oulu.fi

***Abstract*—This paper investigates static properties of laser welded ultra-high-strength (UHS) stainless steel tube. The material of the tube was cold-hardened ultra-high-strength austenitic stainless steel (AISI 301 2H) with a tensile strength of 1.55 GPa. The AISI 301 steel tubes were manufactured by laser welding from two U-shaped parts. For comparison, low strength stainless steel (AISI 304) tubes were also examined in the experiments. The microstructure of the welded joints was studied by optical microscopy. The hardness of the laser weld joint was determined. The strength of the tubes was studied by three-point bending and compression tests. It was observed that the hardness at the HAZ of the AISI 301 joint was 51% lower than that of the base material. HAZ showed new fine grains of austenite phase structure due to the reversion transformation from martensite to austenite. Result showed that the AISI 304 weld had the same hardness as the base material. Three-point bending experiments revealed that the bending strength of the UHS (AISI 301) steel tube was approximately 60% higher than that of low strength AISI 304 steel tube. The location of the weld relative to the direction of the compressive force had a significant effect on the compressive strength of the UHS (AISI 301) steel tube.**

Keywords—ultra-high-strength steel, bending strength, compression strength, laser welding, steel tube

I. Introduction

The effects of climate change are forcing industry to find new ways to reduce the weight of vehicles and thus reduce emissions. The reduction of weight is very important, especially in vehicle structures, where lower fuel consumption and higher load carrying efficiency are particularly significant. Ultra-high-strength (UHS) steels can be utilized in structures that require weight reduction. Using UHS steels, cost-effective structures can be manufactured using new manufacturing methods such as laser welding. The good static load carrying capacity of UHS steels promotes their use in vehicles.

Stainless steels are commonly used in structures because of their good corrosion resistance [1]. Stainless steels, especially the austenitic grades, offer very high ductility and impact resistance. UHS stainless steels can also be utilized in structures that require strength [2]. The strength of austenitic stainless steels can be enhanced by cold-hardening due to the strain hardening of the material. By modifying the chemical composition of the stainless steel, the strength of the steel can also be improved [3]. In welded structures made of cold-hardened austenitic stainless steels, the considerable softening of the heat-affected-zone (HAZ) must be taken into account [4], [5].

Tube structures have excellent strength properties [6]–[9]. In tubes made of UHS steels, the wall thickness can be reduced, and the strength of the structure can still be maintained [10]. Tube structures can also be used in vehicles to absorb kinetic energy during impact [11]. Laser welding is a very good method in the manufacture of tubes because it has good properties such as low heat input, narrow HAZ, low distortion, narrow bead width and cost effectiveness as compared to conventional welding methods [12]. One of the main advantages of laser welding in tube welding is easy automation of the welding process.

There is a little information whether laser welded UHS cold-hardened austenitic stainless steel tubes can be utilized in vehicle structures. The characteristic of cold-hardened austenitic stainless steel is that the welds are considerably softer than the base material, which can affect the strength of the structure [4], [5]. This paper investigates the static properties of UHS steel tubes. Commercially manufactured tubes are used as a reference. The properties of the UHS steel tubes are studied by bending and compression tests. Hardness measurements of laser welds are also performed.

II. Experimental Methods

A. Material of the tube and manufacturing process of the test samples

The material of the UHS steel tube was 2 mm thick cold-hardened austenitic stainless steel AISI 301 2H. The material of the low-strength steel (LS steel) tube was austenitic stainless steel AISI 304. The mechanical properties of the test materials are shown in Table I. The AISI 301 steel plates were bent into a U-shape with a press brake. The U-shaped plates were joined together by laser welding as seen from Fig 1a. Sectional dimensions of the tube were 50 x 50 x 2 mm. The length of the sample for three-point bending was 700 mm. A 100 mm long tube was used in the compression tests.

TABLE I. Mechanical properties of the materials

Material	YS	UTS	Elongation	Hardness
	[MPa]	*[MPa]*	*[%]*	*[HV0.2]*
AISI 301	1280	1550	14.8	502
AISI 304	479	722	42.2	258

B. *Laser welding*

A Yb:YAG diode-pumped disc laser (Trumpf HLD-4002) was used for laser welding of the tubes. The beam quality of the laser was 8 mm*mrad and the wavelength of the laser was 1030 nm. In the welding the focal distance of the optics was 300 mm, and the beam diameter on the surface of the tube was 0.3 mm. The maximum power of the laser source is 4 kW. The focal point was 1 mm below the surface of tube. The laser welding of the tube was performed with power of 3 kW and welding speed was 6 m/min. Argon shielding gas was used in the laser welding of the tube to prevent oxidation and flow rate was 30 l/min.

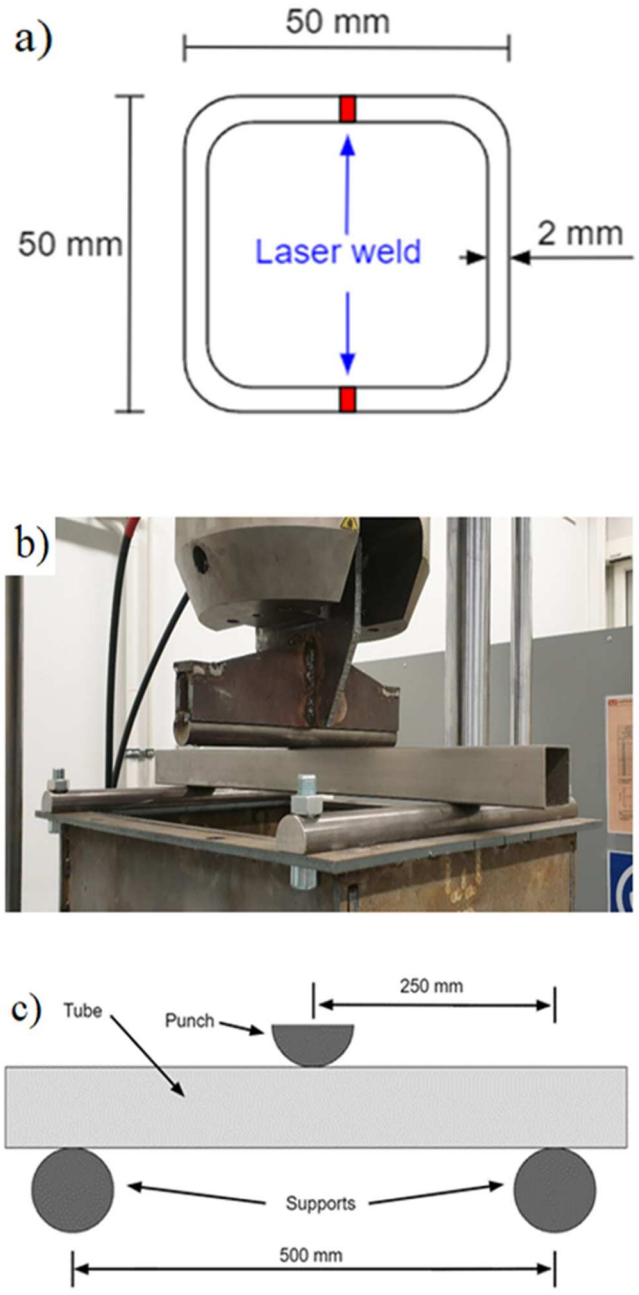

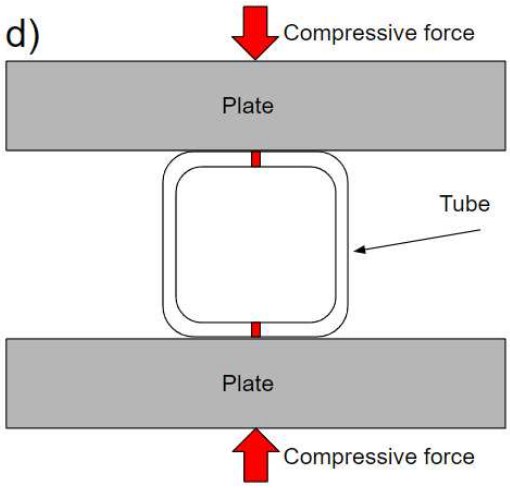

Fig. 1. (a) Dimensions of the test tubes, (b) Test arrangement of the three-point bending test, (c) schematic diagram of the three-point bending test and (d) schematic diagram of the compression test.

C. *Mechanical testing*

Instron 8802 servo-hydraulic loading machine was employed in the three-point bending and compression tests. The force and displacement were measured by the loading cell of the loading machine and the results were recorded. The bending tests were performed at a loading speed of 1 m/min. The setup for three-point bending tests is shown in Fig. 1b. Radius of the punch and supports was 25 mm. The span between supports was 500 mm as seen from Fig 1c. Each bending experiment was repeated with 5 test tubes. In the experimental arrangement of the compression tests, the tube was compressed between two 20 mm thick plates as shown in Fig 1d. The compression tests were performed at a loading speed of 0.5 m/min. Each compression test was repeated 5 times.

Static strength properties for the base materials of the test tubes were determined using Instron 8802 servo-hydraulic loading machine at a constant loading rate of 1.0 mm/min. Tensile tests were carried out according to the standard ASTM E8/8M. Tensile specimens with a gauge length of 75 mm and width of 12.5 mm were used. Vickers microhardness tests were conducted on the cross-section of the laser weld using a Struers Duramin 300-a Vickers hardness tester with a test load of 0.2 kg. The distance between the measurement points was 0.1 mm. Hardness measurements were repeated 3 times and the standard deviation was 10.1 HV. The microstructure of the welded joints was studied by optical microscopy.

III. Results and Discussion

A. *Hardness measurements and microstructure of the weld*

Microstructure of the AISI 301 weld can be seen in Fig 2. and Fig. 3 shows the hardness profile across the weld metal AISI 301. It was observed that the hardness of the FZ is significantly lower than that of the BM, i.e., ~50% lower. Since the hardness values of the BM and the FZ are 502 ± 10.1 HV and 246 ± 10.1 HV, respectively. The high hardness of the BM is attributed to the hard matrix of the of the cold-worked BM, which is predominantly martensite. It is established that the cold deformation of the metastable AISI 301 induces the martensitic

transformation [13]. Fig. 2(a) displays the strain-induced martensite (black regions) in the BM. However, upon welding processing and due to the heat transfer, the HAZ shows new fine grains of austenite phase structure due to the reversion transformation from martensite to austenite, Fig. 2(b). This reversion mechanism has been reported in several publications, e.g. [14]. Fig. 2(c) shows the microstructure of the FZ. It is observed that the microstructure of the FZ is various showing elongated grains with mainly austenitic microstructure.

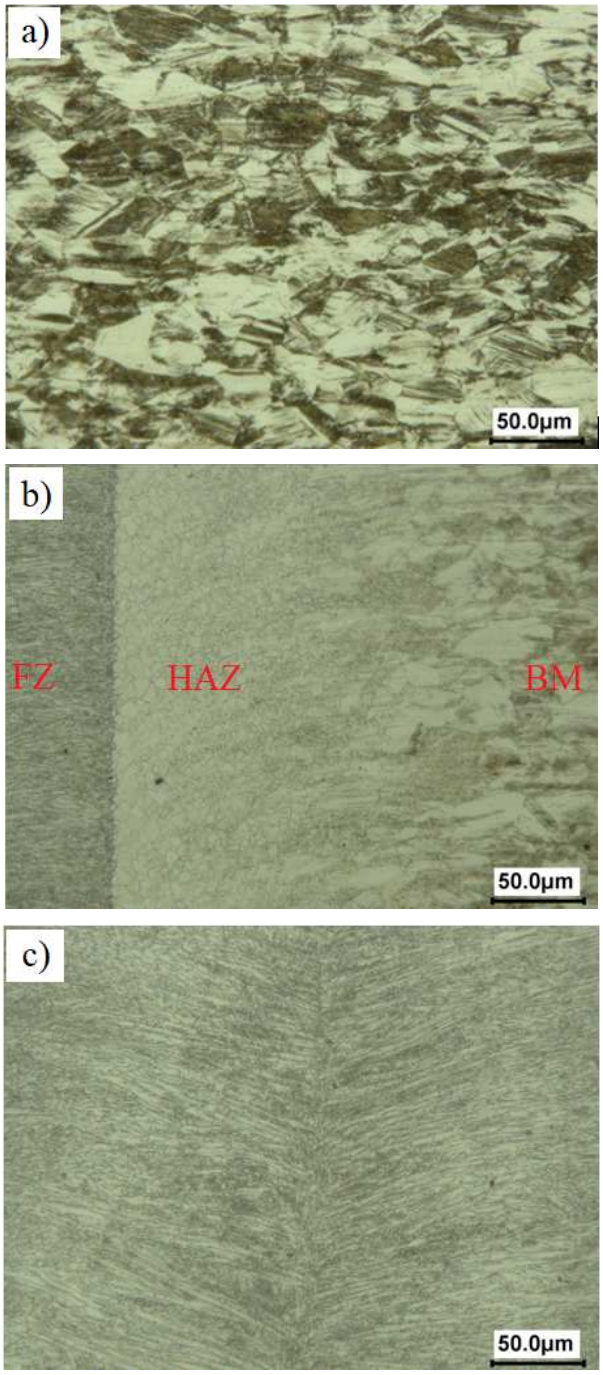

Fig. 2. Microstructure of the different regions at the AISI 301 weldment (a) Base metal, (b) Heat-affected-zone, (c) Fuzion zone.

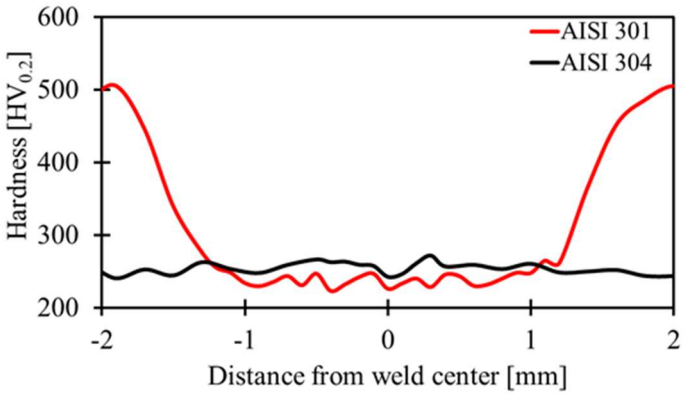

Fig. 3. Hardness profiles of the welds.

B. Bending tests

The UHS steel tube was examined by three-point bending tests and the results were compared with the LS steel tube used as a reference. As seen from Fig. 4a., when testing the UHS steel tube, the loading force increased linearly, and the force peaked at 42.7 kN as the displacement was increased to 11.3 mm. The loading force decreased after the bending collapse. In the case of LS steel tube, the loading force peaked at 26.7 kN when displacement was at 6.8 mm. Based on the results, bending strength of the UHS steel tube was approximately 60% higher than that of LS steel tube. The experiments revealed that the location of the weld in relation to the bending direction had no effect on the bending strength of the UHS steel tube.

Fig. 4b, c and d show typical deformed shapes for the test tubes as a result of a bending test. The bending test of the tubes was performed so that the displacement at the center of the tube was at most 25 mm. As can be seen in Fig. 4b, the tubes underwent a permanent deformation, but no damage occurred to the surface of the tube. A U-shaped deformation occurred in both tubes as seen in Fig 4c. A U-shaped pattern is formed due to the relatively small radius of the punch. Fig. 4b shows that the laser weld was not damaged in the bending test. Based on the bending test, the laser weld does not weaken the strength of the tube, so that damage would occur from the weld.

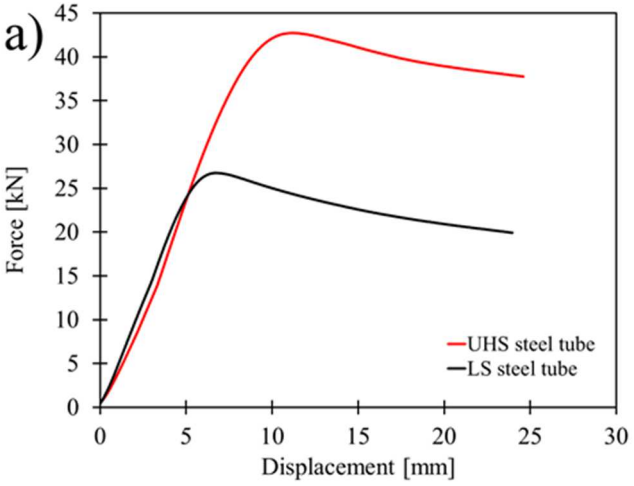

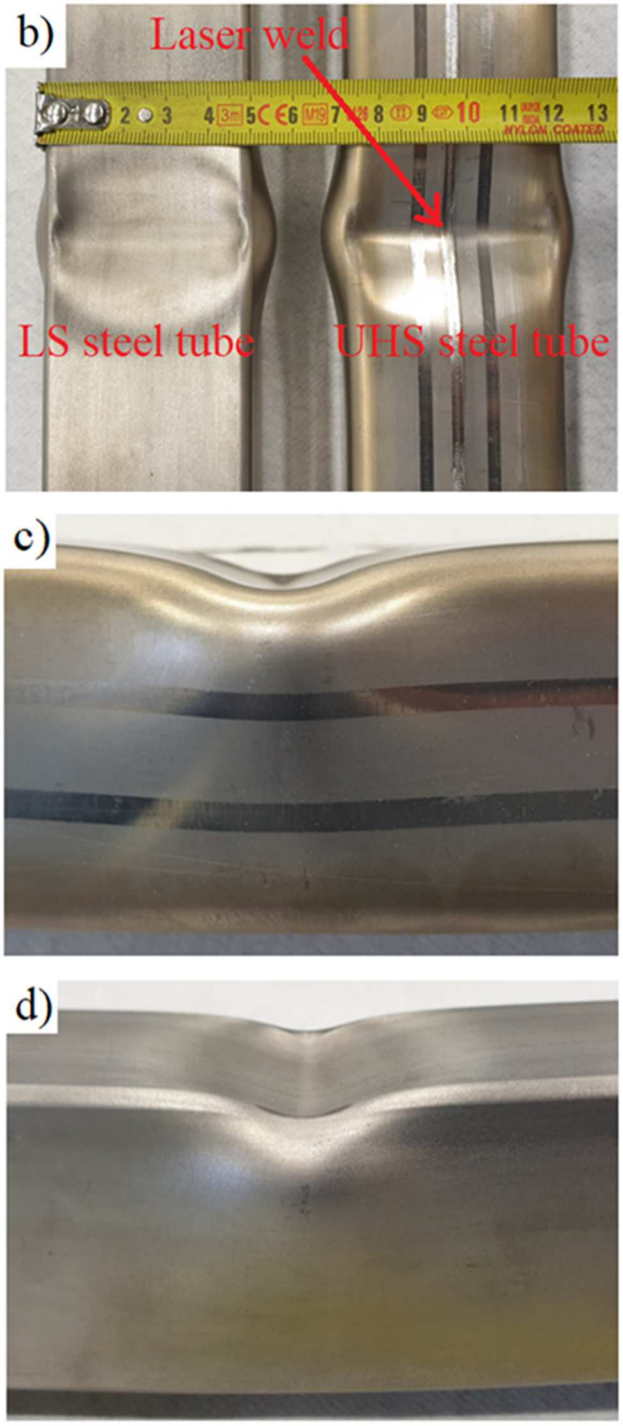

Fig. 4. (a) Bending strengths of the tubes, (b) Deformed tubes after bending test, (c) Deformed shape of UHS steel tube and (d) Deformed shape of LS steel tube.

C. *Compression tests*

Compression tests were performed to determine whether the location of the weld relative to the direction of the load affected the load carrying capacity of the tube. The compression test results indicated that the highest compressive strength value with UHS steel tube was obtained when the weld was parallel (W-P) to the compressive force. In this case, the maximum compressive force was approximately 70.8 kN as seen from Fig. 5. With the weld on the neutral axis (W-NA), the maximum compressive force was 55.6 kN.

The results show that in the UHS steel tube compression test, the location of the weld relative to the direction of the compressive force had a significant effect on the compressive strength of the UHS steel tube. When the weld was on the neutral axis (W-NA), the compressive strength of the UHS steel tube was 21.4% lower than when the weld was parallel to the compression direction.

As shown in Fig. 5., the location of the weld with LS steel tube relative to the compression direction had no significant effect on the strength of the LS steel tube. The maximum compressive force with LS steel tube was approximately 56 kN. The result is in accordance with the fact that weld of LS steel is uniformly hard, as the hardness measurements showed.

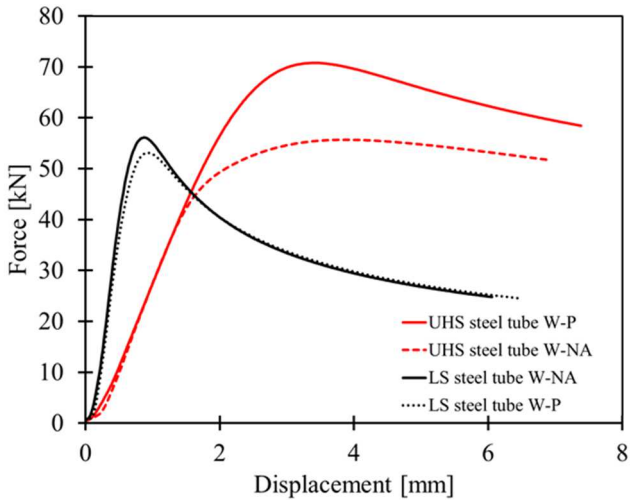

Fig. 5. Compressive strengths of the tubes.

IV. Conclusions

This paper investigated static properties of laser welded ultra-high-strength stainless steel tube (UHS steel tube). The material of the UHS steel tube was cold-hardened AISI 301 2H with a tensile strength of 1.55 GPa. In the paper, a low-strength tube made of AISI 304 steel was examined for comparison. According to the results the following conclusions can be drawn:

- Significant softening was observed in the weld metal of AISI 301 steel. The hardness at the weld metal (including HAZ) of the AISI 301 joint was 51% lower than that of the base material. The AISI 304 weld metal had the same hardness as the base material.
- Maximum bending force of the UHS steel tube was 42.7 kN. Result showed that bending strength of the UHS steel tube was approximately 60% higher than that of LS steel tube.
- The experiments showed that the location of the weld in relation to the bending direction had no effect on the bending strength of the UHS steel tube.
- The experiments showed that the laser welds were not damaged in the bending test. Based on the bending test,

the laser weld does not weaken the strength of the tube, so that damage would occur from the weld.

- The compression test results showed that the highest compressive strength value with UHS steel tube was obtained when the weld was parallel to the compressive force. The maximum compressive force was approximately 70.8 kN.
- The location of the weld relative to the direction of the compressive force had a significant effect on the compressive strength of the UHS steel tube. The weld on the neutral axis, the compressive strength of the UHS steel tube was 21.4% lower than when the weld was parallel to the compression direction. This is due the weld metal is considerably softer than the base material.
- Based on the tests performed, laser welded UHS steel tubes are suitable for vehicle structures, but the softening caused by the weld must be taken into account in the design of the structures.

ACKNOWLEDGMENTS

The authors would like to acknowledge the financial support received from the European Union (European regional development fund), City of Nivala, Nivala industrial park Ltd, NIHAK Nivala-Haapajarvi region registered association. The industrial companies Wärtsilä Finland Oyj, SSAB Europe Oyj, HT Laser Oy and Randax Oy have participated in this research work.

REFERENCES

[1] A. Gnanarathinam, D. Palanisamy, N. Manikandan, A. Devaraju and D. Arulkirubakaran, "Comparison of corrosion behavior on laser welded austenitic stainless steel," *Materials Today: Proceedings*, vol. 39, pp. 649–653, 2021.

[2] E. Ellobody, "Buckling analysis of high strength stainless steel stiffened and unstiffened slender hollow section columns," *Journal of Constructional Steel Research*, vol. 63, pp. 145–155, 2007.

[3] L. Gardner, A. Talja and N. R. Baddoo, "Structural design of high-strength austenitic stainless steel," *Thin-Walled Structures*, vol. 44, pp. 517–528, 2007.

[4] A. Järvenpää, M. Jaskari, M. Keskitalo, K. Mäntyjärvi and P. Karjalainen, "Microstructure and mechanical properties of laser-welded high-strength AISI 301LN steel in reversion-treated and temper-rolled conditions," *Procedia Manufacturing*, vol. 36, pp. 216–223, 2019.

[5] M. Hietala, A. Järvenpää, M. Keskitalo, M. Jaskari and K. Mäntyjärvi, " Tensile and fatigue properties of laser-welded ultra-high-strength stainless spring steel lap joints," *Procedia Manufacturing*, vol. 36, pp. 131–137, 2019.

[6] Z. Huang and X. Zhang, "Three-point bending collapse of thin-walled rectangular beams," *International Journal of Mechanical Sciences*, vol. 144, pp. 461–479, 2018.

[7] F. Gusella and M. Orlando, "Analysis of the dissipative behavior of steel beams for braces in three-point bending," *Engineering Structures*, vol. 244, p. 112717, 2021.

[8] T. H. Kim and S. R. Reid, "Bending collapse of thin-walled rectangular section columns," Computers & Structures, vol. 79, pp. 1897–1911, 2001.

[9] Z. Huang, X. Zhang and X. Fu, "On the bending force response of thin-walled beams under transverse loading," *Thin-Walled Structures*, vol. 154, p. 106807, 2020.

[10] F. Javidan, A. Heidarpour, X. L. Zhao and J. Minkkinen, "Application of high strength and ultra-high strength steel tubes in long hybrid compressive members: Experimental and numerical investigation," *Thin-Walled Structures*, vol. 102, pp. 273–285, 2016.

[11] Z. Huang, X. Zhang and Z. Wang, "Transverse crush of thin-walled rectangular section tubes," *International Journal of Mechanical Sciences*, vol. 134, pp. 144–157, 2017.

[12] W. Guo, D. Crowther, J.A. Francis, A. Thompson and L. Li, "Process-parameter interactions in ultra-narrow gap laser welding of high strength steels," *The International Journal of Advanced Manufacturing Technology*, vol. 84, pp. 2547–2466, 2016.

[13] A. Järvenpää, S. Ghosh, A. Khosravifard, M. Jaskari and A. Hamada, "A new processing route to develop nano-grained structure of a TRIP-aided austenitic stainless-steel using double reversion fast-heating annealing," *Materials Science and Engineering*: A, vol. 808, p. 140917, 2021.

[14] A. Hamada, A. Khosravifard, S. Ghosh, M. Jaskari, A. Järvenpää and P. Karjalainen, "High-speed erichsen testing of grain-refined 301LN austenitic stainless steel processed by double-reversion annealing," *Metallurgical and Materials Transactions A*, 2022.